# Ternary copolymers containing 3,4-dicyanothiophene for efficient organic solar cells with reduced energy loss

Yue Zhang[a], Langheng Pan[a], Zhongxiang Peng[c], Wanyuan Deng[a], Bo Zhang[a,b], Xiyue Yuan[a], Zhili Chen[a,b], Long Ye[c], Hongbin Wu[a], Xiang Gao[b,*], Zhitian Liu[b,*], Chunhui Duan[a,*], Fei Huang[a] and Yong Cao[a]

[a] Institute of Polymer Optoelectronic Materials and Devices, State Key Laboratory of Luminescent Materials and Devices, South China University of Technology, Guangzhou 510640, China

[b] Hubei Engineering Technology Research Center of Optoelectronic and New Energy Materials, Wuhan Institute of Technology, Wuhan, 430205, China

[c] School of Materials Science and Engineering, Tianjin University, Tianjin 300350, P. R. China

* Corresponding author.
E-mail addresses: xgao@wit.edu.cn (X. Gao), able.ztliu@wit.edu.cn (Z. Liu), duanchunhui@scut.edu.cn (C. Duan)

## Contents

**1. General information and characterizations**

1,3-Bis(5-bromothiophen-2-yl)-5,7-bis(2-ethylhexyl)-4H,8H-benzo[1,2-c:4,5 c']dithiophene-4,8-dione (BDD-2Br) and (4,8-bis(5-(2-ethylhexyl)-4-fluorothiophen-2-yl)benzo[1,2-b:4,5-b']dithiophene-2,6 diyl)bis(trimethylstannane) (BDT-F-2Sn) were purchased from SunaTech Inc. and Derthon OPV Co LTD, respectively. Y6-BO (Derthon OPV Co LTD), PDINO (Solarmer Materials Inc.), and solvents used in experiments were purchased from commercial sources (Sigma Aldrich, Acros, Stream, or Alfa Aesar) and used as received unless otherwise indicated. Tetrahydrofuran was distilled over sodium and benzophenone.

The $^1$H and $^{13}$C NMR were measured on a Bruker AV-400 MHz spectrometer with tetramethylsilane (TMS) as the internal reference. Molecular weights of the polymers

were determined using an Agilent Technologies PL-GPC 220 high temperature chromatograph in 1,2,4-trichlorobenzene at 140 °C using a calibration curve of polystyrene standards. UV-vis absorption spectra of the polymer in chlorobenzene solutions and in films were recorded on a SHIMADZU UV-3600 spectrophotometer. The square wave voltammetry (SWV) measurements were conducted on a CHI 600D electrochemical workstation in solution of tetrabutylammonium hexafluorophospate ($Bu_4NPF_6$, 0.1 M) in acetonitrile at a scan rate of 50 mV $s^{-1}$. A platinum electrode coated with polymer film, a platinum wire, and an $Ag^+/AgCl$ electrode were used as the working electrode, counter electrode, and reference electrode, respectively. AFM images were obtained using a Bruker Multimode 8 Microscope AFM in tapping-mode. TEM images were obtained using a JEM-2100F instrument. Grazing incidence wide-angle X-ray scattering (GIWAXS) experiments were carried out on a Xenocs Xeuss 2.0 system with an Excillum MetalJet-D2 X-ray source operated at 70.0 kV, 2.8570 mA, and a wavelength of 1.341 Å. The grazing-incidence angle was set at 0.20°. Scattering pattern was collected with a DECTRIS PILATUS3 R 1M area detector. The raw GIWAXS data were analyzed using Igor 6.37 with a modified NIKA package.

## 2. Synthetic procedures and characterizations

*4,4''-Didodecyl-(2,2':5',2''-terthiophene)-3',4'-dicarbonitrile (2)*: A mixture of 2-(tri-n-butylstannyl)-4-dodecylthiophene (1.62 g, 3 mmol), and compound 1 (250 mg, 0.856 mmol) was dissolved in 20 mL DMF. After being purged by argon twice, $Pd(PPh_3)_4$ (148.43 mg, 0.128 mmol) was added into the solution and then the reaction mixture was purged by argon twice again. The reaction was stirred at 80 °C overnight. After removal of the solvent, the product was purified by silica gel chromatography using dichloromethane: petroleum ether (1:1) solvent mixture as the eluent, which was further purified by recrystallization from the mixture of methanol and tetrahydrofuran (329 mg, yield = 60.5%). $^1H$ NMR (400 MHz, Chloroform-d) δ 7.493 (d, *J* = 1.2 Hz, 2H), 7.102 (q, *J* = 1.2 Hz, 2H), 2.649 − 2.611 (t, *J* = 7.6 Hz, 4H), 1.655 − 1.600 (m, 4H), 1.321 − 1.262 (m, 36H), 0.896 − 0.862 (m, 6H). $^{13}C$ NMR (100 MHz, $CDCl_3$) δ 145.26, 145.15, 130.91, 129.72, 124.13, 112.95, 105.95, 31.92, 30.37, 30.32, 29.67, 29.65, 29.57, 29.40, 29.36, 29.23, 22.70, 14.13.

*5,5''-Dibromo-4,4''-didodecyl-(2,2':5',2''-terthiophene)-3',4' dicarbonitrile (3)*: A mixture of compound 2 (127 mg, 0.2 mmol), and NBS (72.97 mg, 0.41 mmol) in the mixed solvent of chloroform (11 mL) and acetate acid (4 mL) was stirred at 50 °C for 18 hours. The reaction was cooled to room temperature, quenched by deionized water, and then extracted with dichloromethane. The organic layer was dried over magnesium sulfate. After removing the solvent, the crude product was subjected to column chromatography of silica gel using dichloromethane: petroleum ether = (1:1) solvent mixture as the eluent to afford a yellow solid, which was further purified by recrystallization from the solvent mixture of methanol and tetrahydrofuran to give the title compound 3 (100 mg, yield = 63%). ^{1}H NMR (400 MHz, Chloroform-d) δ 7.323 (s, 2H), 2.604 – 2.566 (t, $J$ = 7.6 Hz 4H), 1.638 − 1.566 (m, 2H), 1.37 – 1.25 (m, 36H), 0.91 – 0.85 (m, 6H). ^{13}C NMR (100 MHz, CDCl$_3$) δ 144.23, 144.10, 130.49, 129.39, 114.26, 112.56, 106.25, 31.93, 29.66, 29.64, 29.63, 29.58, 29.54, 29.51, 29.36, 29.35, 29.17, 22.70, 14.13.

*Synthesis of PBDB-TF*: To a degassed solution of 1,3-bis(5-bromothiophen-2-yl)-5,7-bis(2-ethylhexyl)-4H,8H-benzo[1,2-c:4,5-c']dithiophene-4,8-dione (BDD-2Br) (153.35 mg, 0.2 mmol) and (4,8-bis(5-(2-ethylhexyl)-4-fluorothiophen-2-yl)benzo[1,2-b:4,5-b']dithiophene-2,6 diyl)bis(trimethylstannane) (BDT-F-2Sn) (188.11 mg, 0.2 mmol) in anhydrous o-xylene (6 mL) under argon protection, Pd(PPh$_3$)$_4$ (4.6 mg, 0.004 mmol) was added. The mixture was then stirred at 110 ℃ for 12 hours. After that, 2-(tributylstannyl)thiophene and 2-bromothiophene were sequentially added to the reaction with a 2 hours interval. After another 2 hours, the reaction was refluxed with an aqueous solution of sodium N,N-diethylcarbamodithioate trihydrate for 2 hours. After cooling to room temperature, the reaction mixture was precipitated in methanol and filtered through a Soxhlet thimble. The polymer was subjected to sequential Soxhlet extraction with methanol, acetone, hexane, dichloromethane and chloroform under argon protection. The chloroform fraction was concentrated under reduced pressure and precipitated in methanol to obtain the polymer (233 mg, yield = 93%). Elemental analysis (EA) calcd, N: 0%, C: 66.85%, H: 6.43%, S: 20.99%. Found, N: 0%, C: 66.56%, H: 6.50%, S: 20.15%.

*Synthesis of PFBCNT10*: To a degassed solution of compound 3 (11.89 mg, 0.015 mmol), 1,3-bis(5-bromothiophen-2-yl)-5,7-bis(2-ethylhexyl)-4H,8H-benzo[1,2-c:4,5-c']dithiophene-4,8-dione (BDD-2Br) (103.51 mg, 0.135 mmol) and (4,8-bis(5-(2-ethylhexyl)-4-fluorothiophen-2-yl)benzo[1,2-b:4,5-b']dithiophene-2,6 diyl)bis(trimethylstannane) (BDT-F-2Sn) (141.08 mg, 0.15 mmol) in anhydrous *o*-xylene (6 mL) under argon protection, Pd(PPh$_3$)$_4$ (3.47 mg, 0.003 mmol) was added. The mixture was then stirred at 120 ℃ for 12 hours. After that, 2-(tributylstannyl)thiophene and 2-bromothiophene were sequentially added to the reaction with a 2 hours interval. After another 2 hours, the reaction was refluxed with an aqueous solution of sodium N,N-diethylcarbamodithioate trihydrate for 2 hours. After cooling to room temperature, the reaction mixture was precipitated in methanol and filtered through a Soxhlet thimble. The polymer was subjected to sequential Soxhlet extraction with methanol, acetone, hexane, dichloromethane and chloroform under argon protection. The residue in Soxhlet thimble was dissolved in hot chlorobenzene and filtered afterward. The chlorobenzene fraction was concentrated under reduced pressure and precipitated in methanol to obtain the polymer (182 mg, yield = 99%). Elemental analysis (EA) calcd, N: 0.22%, C: 67.10%, H: 6.53%, S: 20.69%. Found, N: 0.14%, C: 66.91%, H: 6.50%, S: 19.93%.

*Synthesis of PFBCNT20*: The polymerization procedure was the same as that of PFBCNT10 by using the compound 3 (23.79 mg, 0.03 mmol), BDD-2Br (92 mg, 0.12 mmol) and BDT-F-2Sn (141.08 mg, 0.15 mmol) as the monomers to afford the polymer (170 mg, yield = 92%). Elemental analysis (EA) calcd, N: 0.45%, C: 67.34%, H: 6.63%, S: 20.39%. Found, N: 0.37%, C: 67.37%, H: 6.68%, S: 20.03%.

*Synthesis of PFBCNT30*: The polymerization procedure was the same as that of PFBCNT10 by using the compound 3 (35.68 mg, 0.045 mmol), BDD-2Br (80.50 mg, 0.105 mmol) and BDT-F-2Sn (141.08 mg, 0.15 mmol) as the monomers to afford the polymer in chlorobenzene fraction (100 mg, yield = 54%). Elemental analysis (EA) calcd, N: 0.67%, C: 67.59%, H: 6.73%, S: 20.09%. Found, N: 0.58%, C: 67.71%, H: 6.68%, S: 19.73%.

## 3. Device fabrication and characterizations

*Fabrication of organic solar cells*: ITO-coated glass substrates were successively precleaned with isopropanol, detergent, de-ionized water, and isopropanol. Ultrasound was performed for 15 minutes at one time. The substrates were subjected to ultraviolet/ozone treatment for 3 minutes. For devices taken PEDOT:PSS as the hole transporting layer (HTL), 40 nm PEDOT: PSS (Clevios P VP AI4083) was spin-coated onto the plasma-treated ITO substrates and baked at 150 °C for 15 min. The substrates were transferred to a nitrogen-filled glove box. The active layer was spin-coated from a chloroform solution of the corresponding polymer donor and Y6-BO (1:1.2 by weight), giving a thickness of ~100 nm. 1,8-Diiodoctane (DIO) is used as the additive solution. The active layer was thermal-annealed at 100 °C after spin coating. After that, a layer of PDINO was spin-coated from a methanol solution (1 mg mL$^{-1}$) at a spin speed of 3000 rpm for 30 seconds. Finally, a layer of Al (100 nm) was thermally evaporated at a pressure of $4 \times 10^{-7}$ Torr.

*Current density–voltage (J−V) characteristics*: The *J–V* curves were measured on a computer-controlled Keithley 2400 source meter under 1 sun, AM1.5 G spectra from solar simulator (Enlitech, Taiwan), the light intensity was 100 mWcm$^{-2}$ as calibrated by using a China General Certification Centre (CGC) certified reference monocrystal silicon cell (Enlitech), and the irradiation area of solar simulator was $12 \times 12$ cm$^2$. Before the *J–V* test of small area devices, a physical mask containing an aperture with a precise area of 4 mm$^2$ was used to define the device area.

*External quantum efficiency (EQE)*: The external quantum efficiency (EQE) spectra were recorded on a commercial EQE measurement system (Enlitech, QE-R3011, Taiwan).

*Single-carrier devices*: Space-charge-limited-current hole and electron mobilities were acquired through the hole-only devices with a configuration of ITO/PEDOT:PSS/PFBCNTx:Y6-BO/MoO$_3$/Ag and electron-only devices with a configuration of ITO/ZnO/PFBCNTx:Y6-BO/PFN-Br/Ag, respectively. The thickness of the PFBCNTx:Y6-BO blend films is about 150 nm. The dark current densities of the single-carrier devices were measured by applying a voltage between 0 and 5 V using a

computer-controlled Keithley 2400 source meter under $N_2$ atmosphere. The data was analyzed according to the Mott–Gurney law that considers a Poole–Frenkel-type dependence of mobility on the electric field, $$J = \frac{9}{8}\varepsilon_r\varepsilon_0\mu_0\frac{V^2}{d^3}exp(0.891\gamma\sqrt{\frac{V}{d}})$$, where $\varepsilon_0$ is permittivity of free space, $\varepsilon_r$ is the dielectric constant of the polymer which is assumed to be around 3 for the conjugated polymers, $\mu_0$ is the zero-field mobility, V is the voltage drop across the device, $d$ is the film thickness of the active layer, and $\gamma$ is a parameter that describes the strength of the field-dependence effect. The applied voltage is used without correcting for series resistance or built-in voltage, which offers the best fitting of the experimental data following the protocol reported in the literature. The hole and electron mobilities are extracted with the fit parameters at an electric field (E) of $2 \times 10^5$ V $cm^{-1}$ by the Murgatroyd equation $\mu(E) = \mu_0 exp(\gamma\sqrt{E})$.

*FTPS-EQE measurements*: FTPS-EQE measurements were measured by using a NICOLETiS50 (Thermo Fisher Scientific) equipped with a quartz tungsten halogen lamp, high pass filter, and internal detector option. Photocurrents of the photovoltaic devices were amplified by a low-noise current amplifier (SR570), with light modulated by the Fourier transform infrared spectrometer (FTIR). The current signals of the devices were collected based on a feedback system for the output voltage of the current amplifier controlled by the FTIR software. A certified mono-crystal silicon reference cell was used to calibrate the photocurrent spectrum, in order to calculate the external quantum efficiency (EQE) of the photovoltaic devices.

*EL measurement*: The electroluminescence spectra were acquired by a high-sensitivity spectrometer (QE Pro and NIR Quest 512, Ocean Optics), while the external quantum efficiency of EL was determined by measuring the emitted photons in all direction through an integrated sphere by using a calibrated spectrometer (QE Pro, Ocean Optics), with the device injected by an external current/voltage source with constant current density.

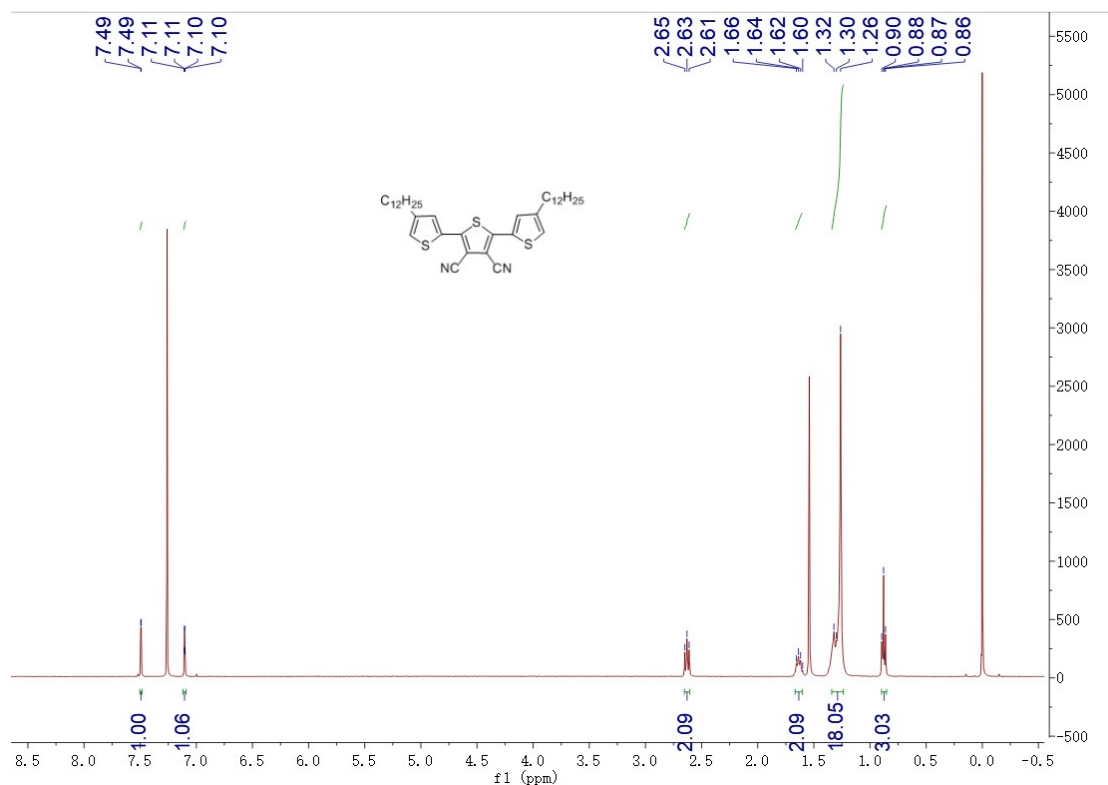## 4. Additional figures and tables
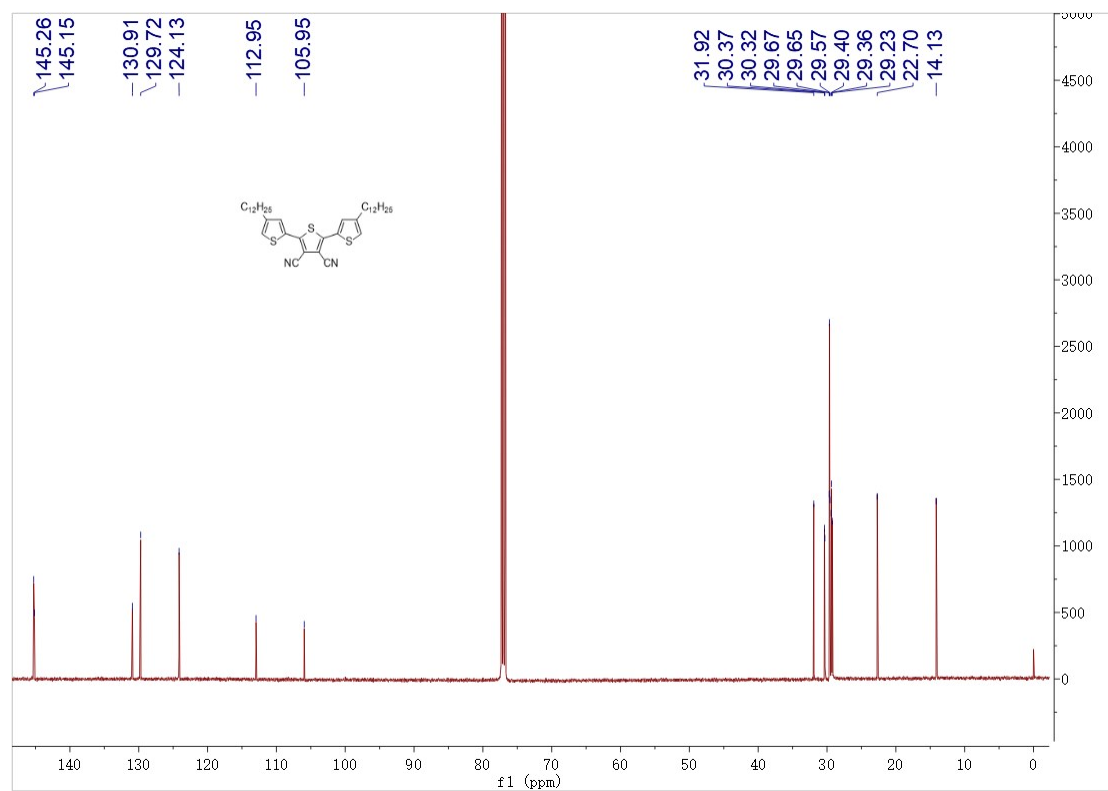


**Figure S1**. $^1H$ NMR spectrum of the compound 2.

**Figure S2.** $^{13}$C NMR spectrum of the compound 2.
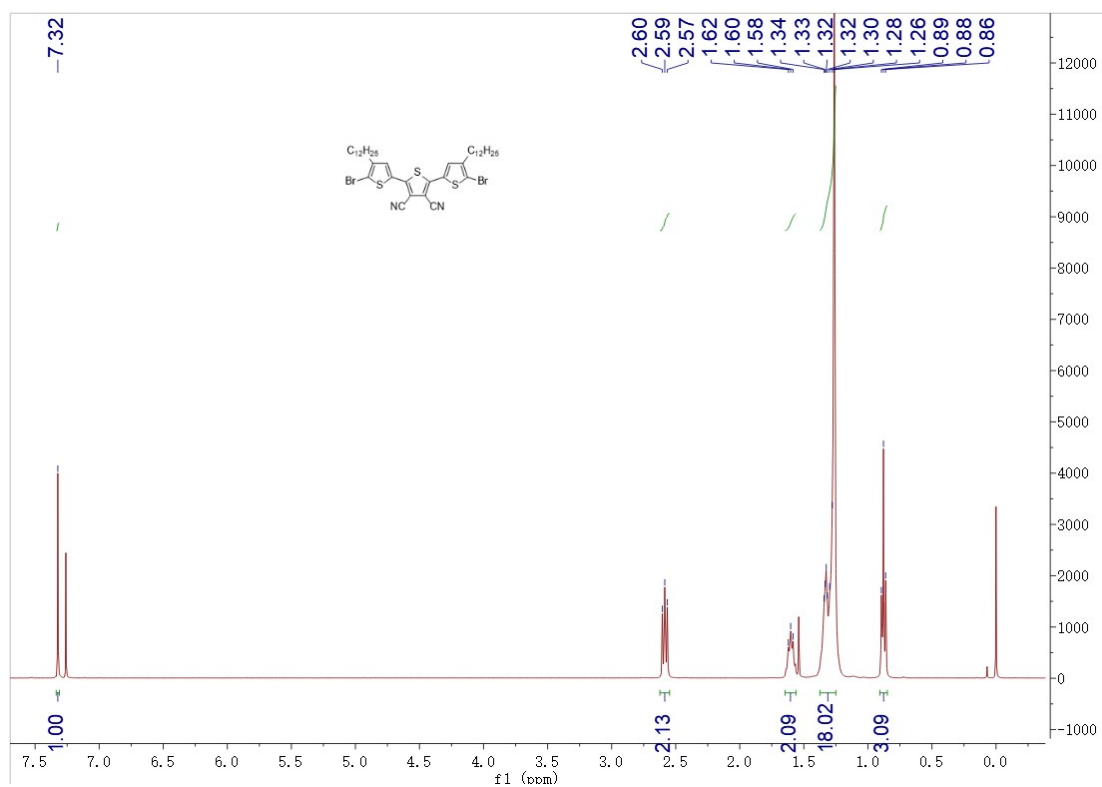


**Figure S3.** $^1$H NMR spectrum of the compound 3.
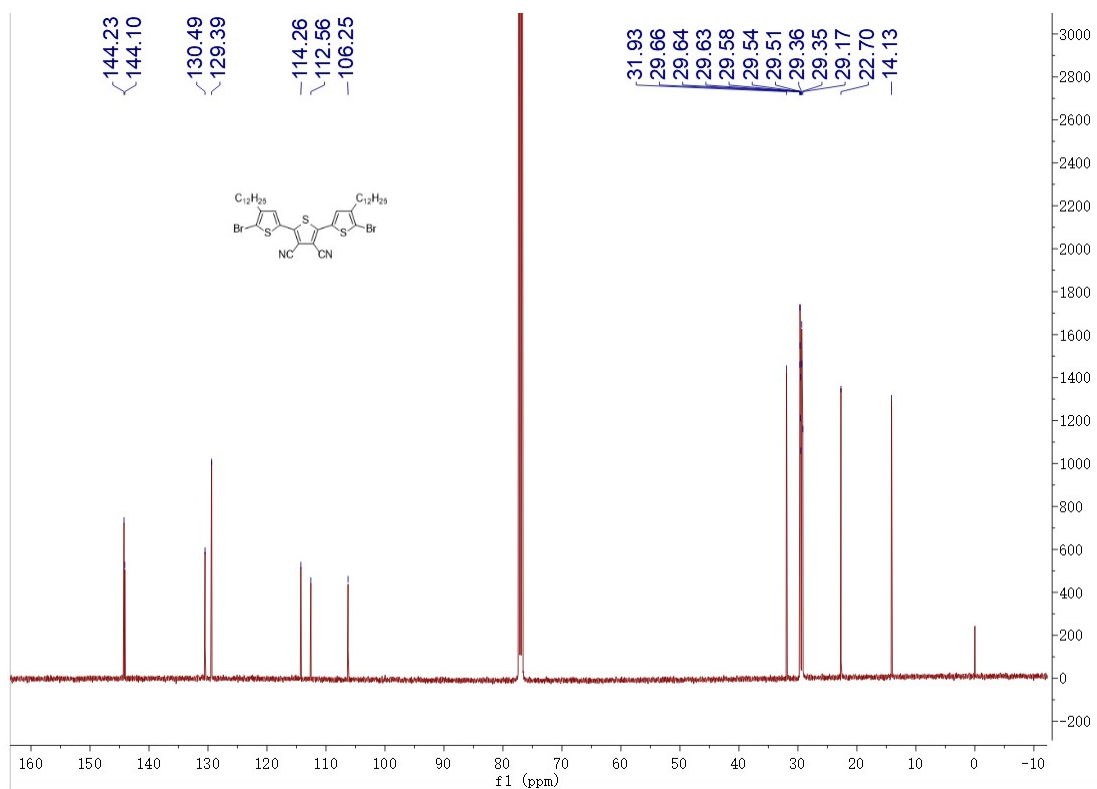


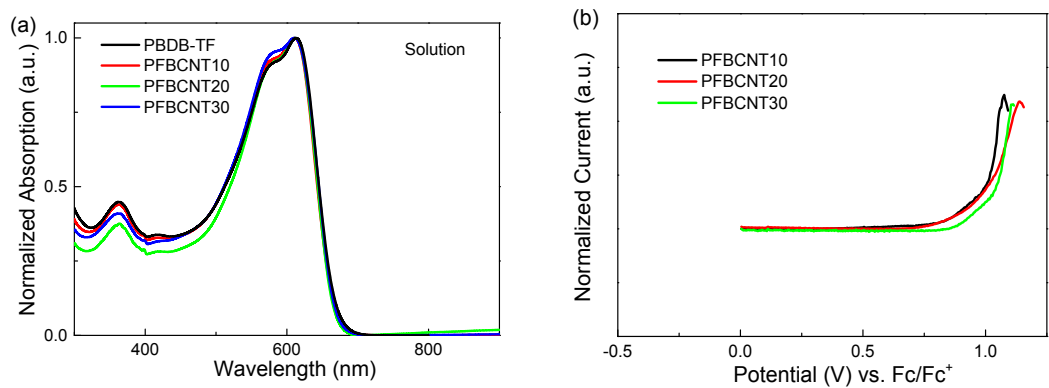**Figure S4.** $^{13}$C NMR spectrum of the compound 3.

**Figure S5.** (a) Normalized UV−vis absorption spectra of polymers in chlorobenzene solution and (b) square wave voltammograms (SWV) measurements of the polymers.
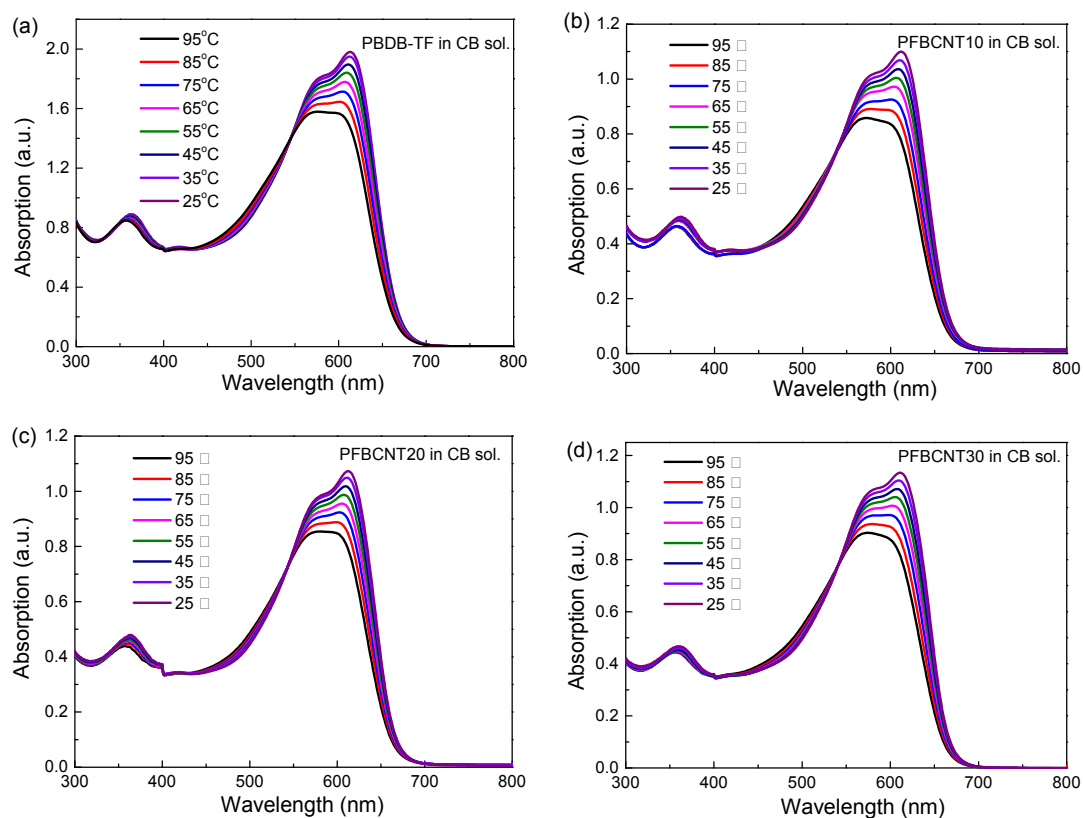


**Figure S6.** Temperature dependent absorption spectra of (a) PBDB-TF, (b) PFBCNT10, (c) PFBCNT20, and (d) PFBCNT30 in dilute CB solution.
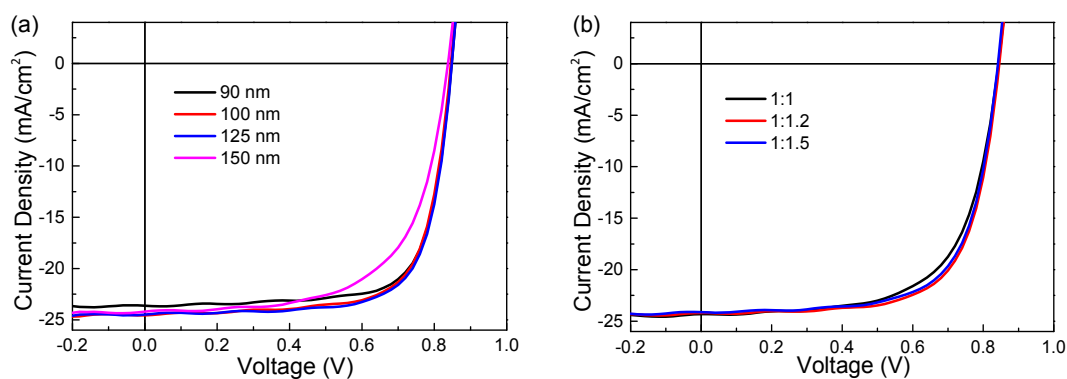
**Figure S7.** Current density–voltage (*J–V*) characteristics of the OSCs based on PFBCNT20:Y6-BO made from (a) active layers with different thickness and (b) with different D:A weight ratios.
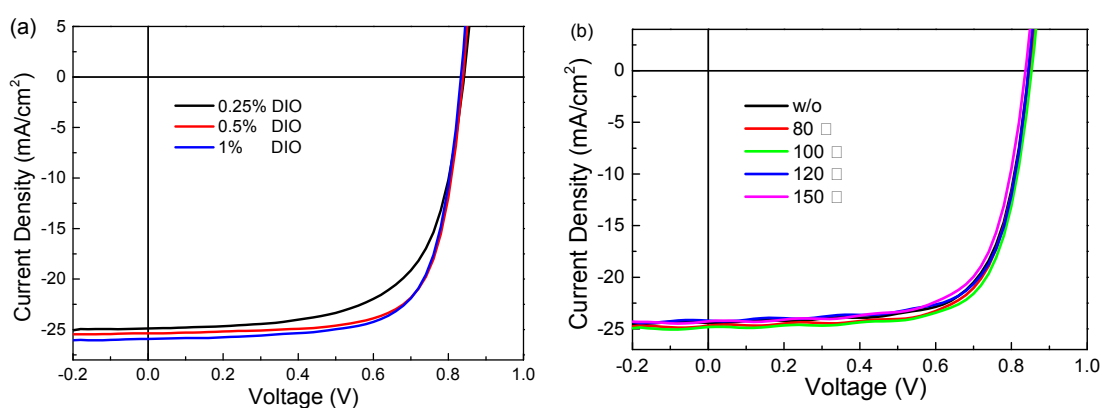


**Figure S8.** Current density–voltage (*J–V*) characteristics of the OSCs based on PFBCNT20:Y6-BO made (a) from CF with different DIO concentrations and (b) after thermal annealing at different temperatures.

**Table S1.** Performance parameters of the OSCs based on PFBCNT20:Y6-BO fabricated from CF+0.5% CN with different concentrations of photovoltaic materials. All the active layers were prepared at a speed of 3000 rpm.

| Concentration (mg/ml) | Thickness | $V_{oc}$ (V) | $J_{sc}$ (mA/cm$^2$) | FF (%) | PCE (%) |
|---|---|---|---|---|---|
| 11.0 | 90 | 0.85 | 23.6 | 73.5 | 14.7 |
| 12.1 | 100 | 0.85 | 24.6 | 71.8 | 14.9 |
| 13.2 | 125 | 0.85 | 24.5 | 72.8 | 15.1 |
| 14.4 | 150 | 0.84 | 24.2 | 63.3 | 12.8 |

**Table S2.** Performance parameters of the OSCs based on PFBCNT20:Y6-BO fabricated from CF+0.5% CN with different D:A weight ratios.

| PFBCNT20:Y6-BO | $V_{oc}$ (V) | $J_{sc}$ (mA cm$^{-2}$) | FF (%) | PCE (%) |
|---|---|---|---|---|
| 1:1 | 0.84 | 24.3 | 65.1 | 13.3 |
| 1:1.2 | 0.85 | 24.2 | 69.2 | 14.1 |

| | | | | |
|---|---|---|---|---|
| 1:1.5 | 0.84 | 24.1 | 68.4 | 13.8 |

**Table S3**. Performance parameters of the OSCs based on PFBCNT20:Y6-BO fabricated from CF with different additives.

| PFBCNT20:Y6-BO | $V_{oc}$ (V) | $J_{sc}$ (mA cm$^{-2}$) | FF (%) | PCE (%) |
|---|---|---|---|---|
| CF+0.5% CN | 0.84 | 25.5 | 71.0 | 15.2 |
| CF+0.5% DIO | 0.84 | 25.8 | 73.8 | 16.0 |

**Table S4.** Performance parameters of the OSCs based on PFBCNT20:Y6-BO fabricated from CF with different DIO concentrations.

| PFBCNT20:Y6-BO | $V_{oc}$ (V) | $J_{sc}$ (mA cm$^{-2}$) | FF (%) | PCE (%) |
|---|---|---|---|---|
| CF+0.25% DIO | 0.84 | 24.9 | 64.7 | 13.5 |
| CF+0.5% DIO | 0.84 | 25.4 | 71.9 | 15.3 |
| CF+1% DIO | 0.83 | 22.6 | 67.4 | 12.6 |

**Table S5**. Performance parameters of the OSCs based on PFBCNT20:Y6-BO after thermal annealing at different temperatures.

| TA | $V_{oc}$ (V) | $J_{sc}$ (mA cm$^{-2}$) | FF (%) | PCE (%) |
|---|---|---|---|---|
| w/o | 0.85 | 24.4 | 70.0 | 14.4 |
| 80 ℃ | 0.85 | 24.7 | 70.5 | 14.7 |
| 100 ℃ | 0.85 | 24.8 | 71.4 | 15.0 |
| 120 ℃ | 0.85 | 24.2 | 70.8 | 14.4 |
| 150 ℃ | 0.84 | 24.3 | 69.2 | 14.0 |

**Table S6**. Performance parameters of the OSCs based on PFBCNT20:Y6-BO with different electron transporting layer. Al electrode is used as the cathode.

| ETL | $V_{oc}$ (V) | $J_{sc}$ (mA cm$^{-2}$) | FF (%) | PCE (%) |
|---|---|---|---|---|
| PDINO | 0.85 | 26.3 | 72.1 | 16.0 |
| PDINN | 0.85 | 26.2 | 70.9 | 15.7 |
| PFN-Br | 0.84 | 25.4 | 69.5 | 14.8 |
| PNDIT-F3N | 0.84 | 25.4 | 73.3 | 15.7 |
| a-ZrAcac | 0.85 | 24.8 | 70.7 | 15.0 |

**Table S7**. Performance parameters of the OSCs with different cathode. PDINO is used as the electron transporting layer.

| Active layer | Cathode | $V_{oc}$ (V) | $J_{sc}$ (mA cm$^{-2}$) | FF (%) | PCE (%) |
|---|---|---|---|---|---|
| PBDB-TF:Y6-BO | Al | 0.81 | 26.0 | 74.5 | 15.7 |
| | Ag | 0.79 | 26.7 | 68.2 | 14.3 |
| PFBCNT20:Y6-BO | Al | 0.83 | 26.0 | 73.5 | 15.9 |
| | Ag | 0.84 | 25.8 | 69.7 | 15.0 |

**Table S8.** Optimization of content of the third component PC$_{71}$BM.

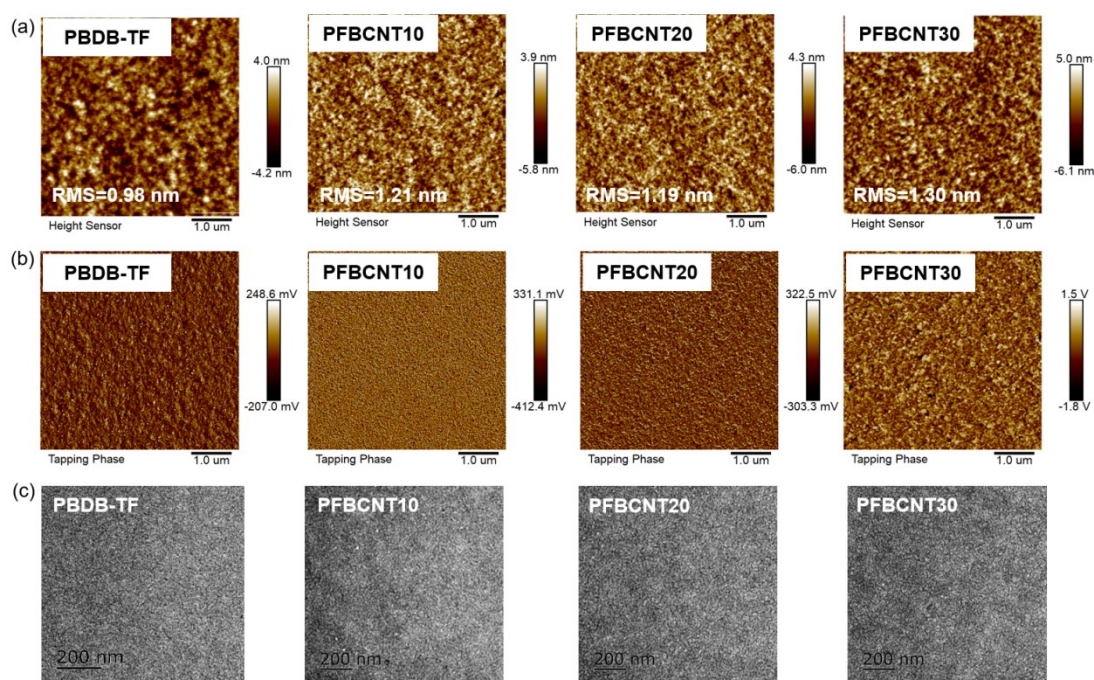| PFBCNT20:Y6-BO:PC$_{71}$BM | $V_{oc}$ (V) | $J_{sc}$ (mA cm$^{-2}$) | FF (%) | PCE (%) |
|---|---|---|---|---|
| 1:1.2:0.2 | 0.84 | 26.4 | 70.2 | 15.6 |
| 1:1:0.2 | 0.85 | 26.6 | 72.8 | 16.6 |
| 1:0.9:0.3 | 0.85 | 24.2 | 73.1 | 15.1 |



**Figure S9**. (a)Tapping-mode AFM height images, (b) AFM phase images, and (c) bright-field TEM images of the blend films of PBDB-TF:Y6-BO, PFBCNT10:Y6-BO, PFBCNT20:Y6-BO and PFBCNT30:Y6-BO, respectively.
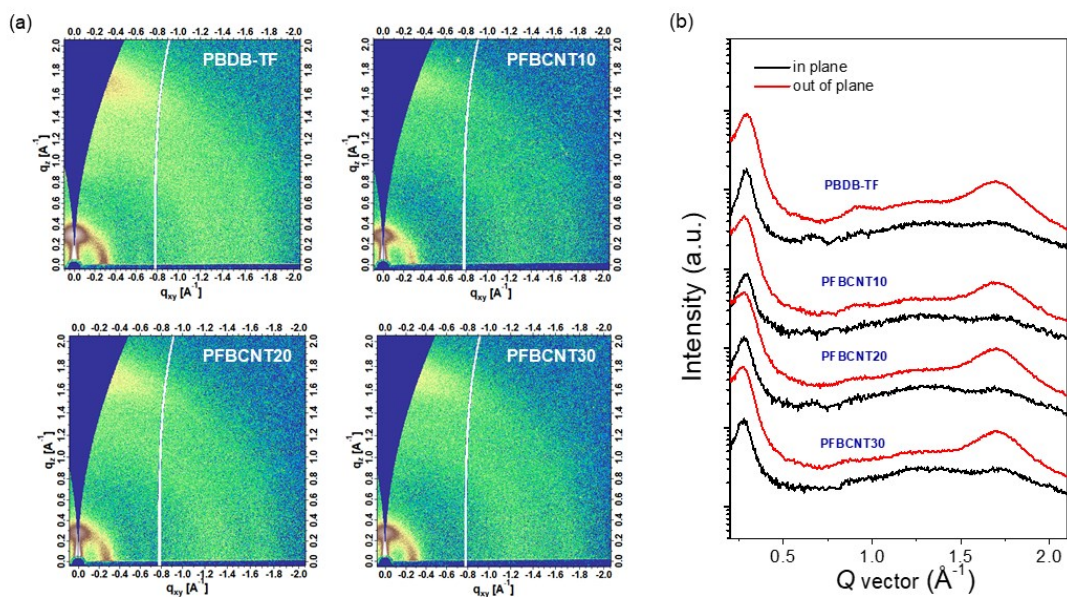
**Figure S10.** (a) Two-dimensional GIWAXS patterns of neat PBDB-TF, PFBCNT10, PFBCNT20 and PFBCNT30. (b) One-dimensional in-plane and out-of-plane profiles of the neat polymers.

**Table S9.** GIWAXS parameters of the pure polymer films.

| Pure films | (010) $q$ position ($\text{Å}^{-1}$) | (010) $d$-spacing (Å) | (010) FWHM ($\text{Å}^{-1}$) | (010) $L_c$ (Å) |
|---|---|---|---|---|
| PBDB-TF | 1.70 | 3.70 | 0.33 | 17.1 |
| PFBCNT10 | 1.71 | 3.67 | 0.32 | 17.7 |
| PFBCNT20 | 1.71 | 3.67 | 0.25 | 22.6 |
| PFBCNT30 | 1.71 | 3.67 | 0.30 | 18.8 |

**Table S10**. GIWAXS parameters of the polymer:Y6-BO blend films.

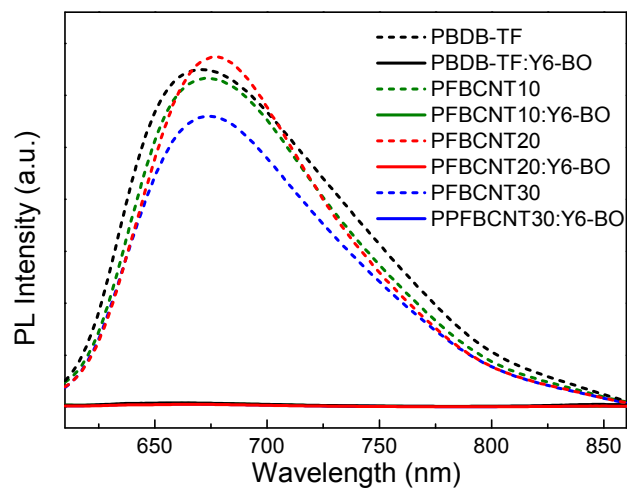| Blend films | | (010) $q$ position ($\text{Å}^{-1}$) | (010) $d$-spacing (Å) | (010) FWHM ($\text{Å}^{-1}$) | (010) $L_c$ (Å) |
|---|---|---|---|---|---|
| PBDB-TF:Y6-BO | PBDB-TF | 1.67 | 3.76 | 0.51 | 11.1 |
| | Y6-BO | 1.74 | 3.61 | 0.21 | 26.9 |
| PFBCNT10:Y6-BO | PFBCNT10 | 1.67 | 3.76 | 0.54 | 10.5 |
| | Y6-BO | 1.75 | 3.59 | 0.21 | 26.9 |
| PFBCNT20:Y6-BO | PFBCNT20 | 1.68 | 3.74 | 0.51 | 11.1 |
| | Y6-BO | 1.75 | 3.59 | 0.21 | 26.9 |
| PFBCNT30:Y6-BO | PFBCNT30 | 1.68 | 3.74 | 0.52 | 10.9 |
| | Y6-BO | 1.76 | 3.57 | 0.21 | 26.9 |

**Figure S11.** The photoluminescence (PL) spectra of the pure polymer films and related blended film.

**Table S11.** PL quenching efficiencies ($\triangle$PL) of the polymer donors in polymer:Y6-BO blends.

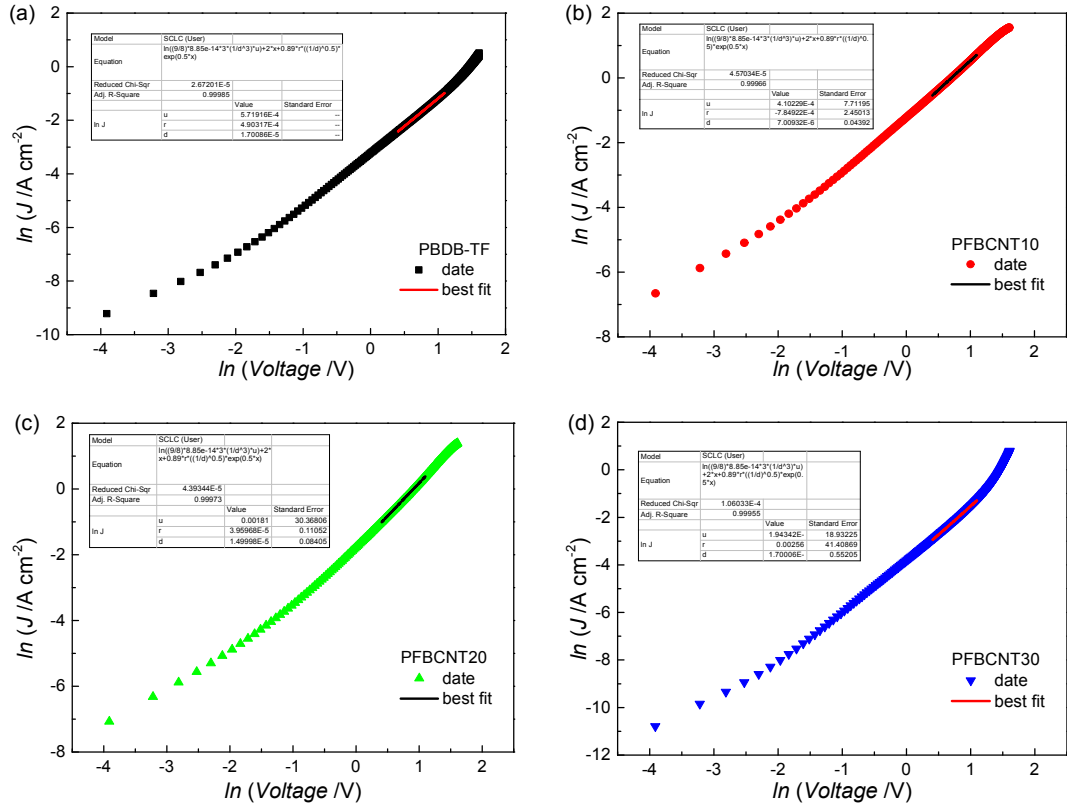| Donor | $\triangle$PL |
|---|---|
| PBDB-TF | 98.8% |
| PFBCNT10 | 98.9% |
| PFBCNT20 | 99.2% |
| PFBCNT30 | 98.7% |

**Figure S12.** Current density versus voltage characteristics of hole-only devices with a configuration of ITO/PEDOT:PSS/polymer/MoO$_3$/Ag plotted in the format of *lnJ ~ lnV*: (a) PBDB-TF, (b) PFBCNT10, (c) PFBCNT20, and (d) PFBCNT30.

**Table S12.** Summary of the derived fitting data for the hole-only devices based on Mott-Gurneys law with field-dependent mobility of the polymers.

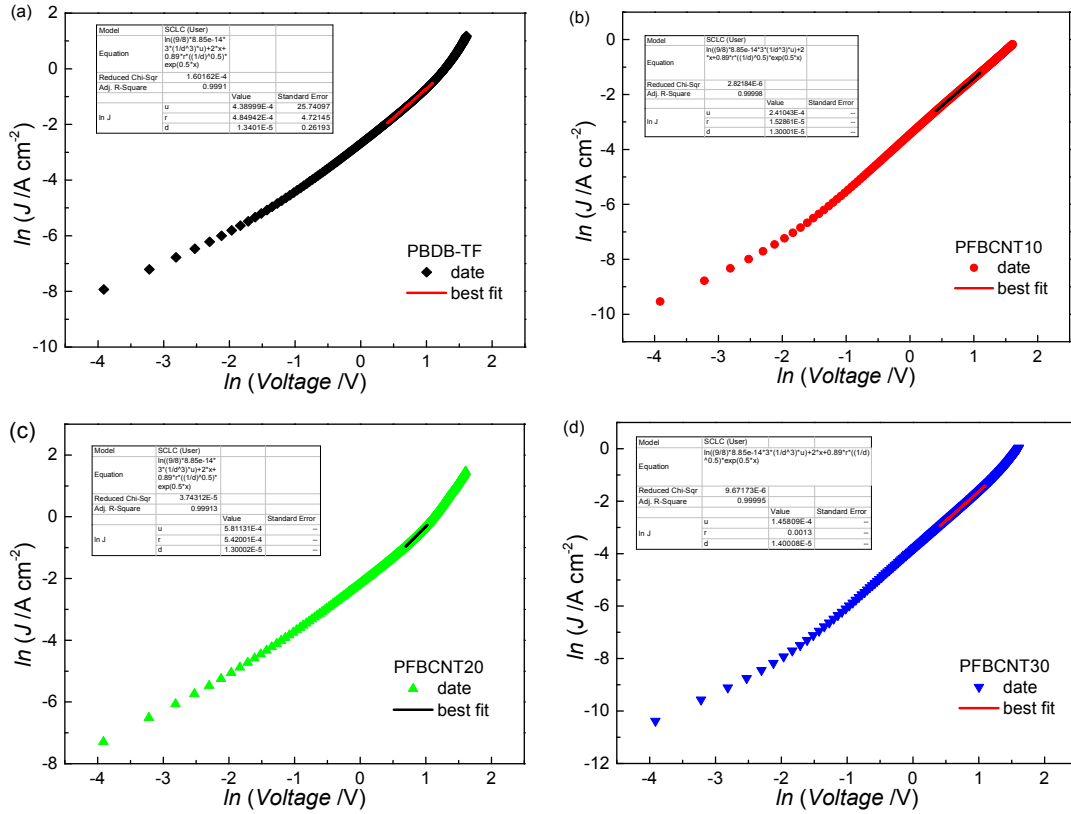| Polymer | Zero-field mobility $\mu_0$ (cm$^2$ V$^{-1}$ s$^{-1}$) | Field-dependence factor $\gamma$ (cm$^{1/2}$ V$^{-1/2}$) | $\mu_h$ at E=2×10$^5$ V cm$^{-1}$ (cm$^2$ V$^{-1}$ s$^{-1}$) |
|---|---|---|---|
| PBDB-TF | 5.72×10$^{-4}$ | 4.90×10$^{-4}$ | 6.77×10$^{-4}$ |
| PFBCNT10 | 4.10×10$^{-4}$ | -7.85×10$^{-4}$ | 2.69×10$^{-4}$ |
| PFBCNT20 | 1.81×10$^{-3}$ | 3.96×10$^{-5}$ | 2.08×10$^{-3}$ |
| PFBCNT30 | 1.94×10$^{-4}$ | 2.56×10$^{-3}$ | 4.68×10$^{-4}$ |

**Figure S13.** Current density versus voltage characteristics of hole-only devices with a configuration of ITO/PEDOT:PSS/polymer:Y6-BO/MoO$_3$/Ag plotted in the format of *lnJ ~ lnV*: (a) PBDB-TF:Y6-BO, (b) PFBCNT10:Y6-BO, (c) PFBCNT20:Y6-BO, and (d) PFBCNT30:Y6-BO blend films.

**Table S13.** Summary of the derived fitting data for the hole-only devices based on Mott-Gurneys law with field-dependent mobility of the polymer:Y6-BO blends.

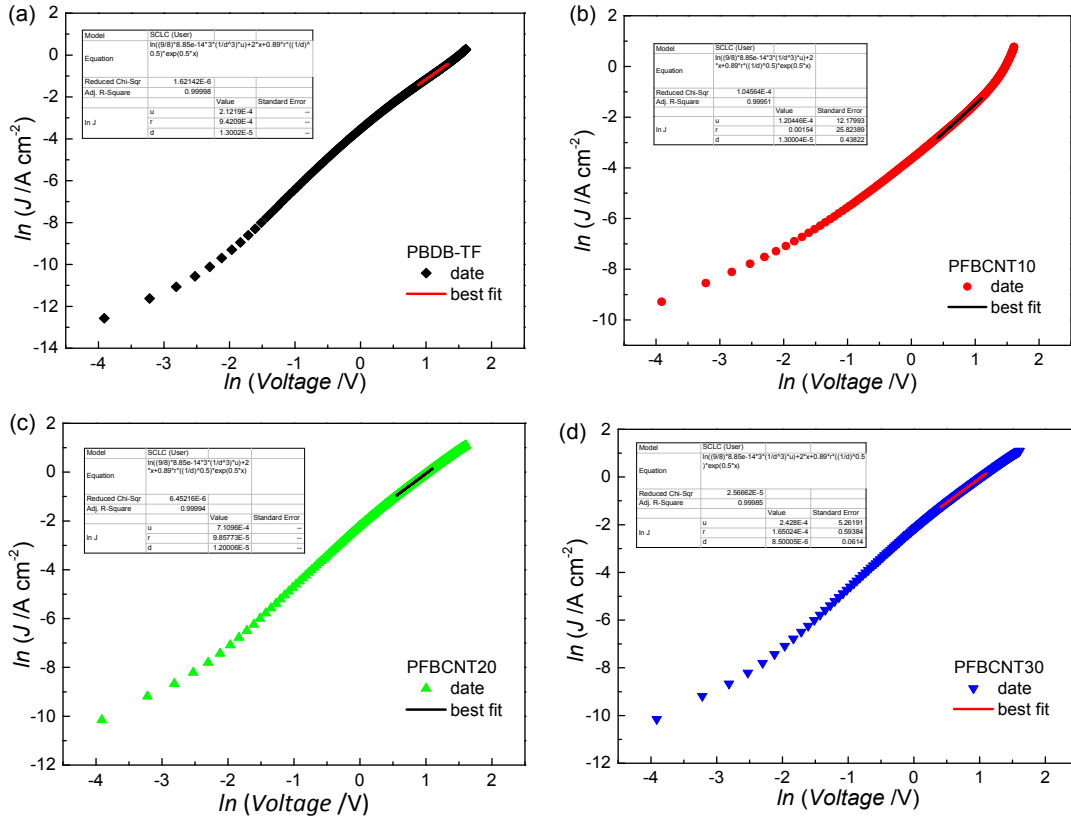| Polymer | Zero-field mobility $\mu_0$ (cm$^2$ V$^{-1}$ s$^{-1}$) | Field-dependence factor $\gamma$ (cm$^{1/2}$ V$^{-1/2}$) | $\mu_h$ at E=2×10$^5$ V cm$^{-1}$ (cm$^2$ V$^{-1}$ s$^{-1}$) |
|---|---|---|---|
| PBDB-TF | 4.39×10$^{-4}$ | 4.85×10$^{-4}$ | 5.31×10$^{-4}$ |
| PFBCNT10 | 2.41×10$^{-4}$ | 1.53×10$^{-5}$ | 2.42×10$^{-4}$ |
| PFBCNT20 | 5.81×10$^{-4}$ | 5.42×10$^{-4}$ | 8.39×10$^{-4}$ |
| PFBCNT30 | 1.46×10$^{-4}$ | 1.30×10$^{-3}$ | 2.39×10$^{-4}$ |

**Figure S14**. Current density versus voltage characteristics of electron-only devices with a configuration of ITO/ZnO/polymer:Y6-BO/PFN-Br/Ag plotted in the format of $lnJ \sim lnV$: (a) PBDB-TF:Y6-BO, (b) PFBCNT10:Y6-BO, (c) PFBCNT20:Y6-BO, and (d) PFBCNT30:Y6-BO blend films.

**Table S14.** Summary of the derived fitting data for the electron-only devices based on Mott-Gurneys law with field-dependent mobility of the polymer:Y6-BO blends.

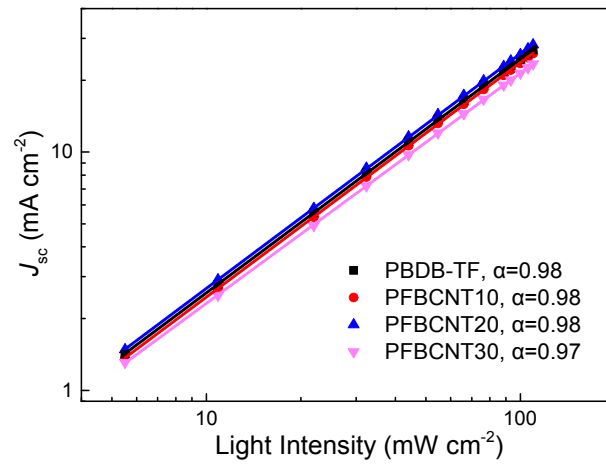| Blend film | Zero-field mobility $\mu_0$ (cm$^2$ V$^{-1}$ s$^{-1}$) | Field-dependence factor $\gamma$ (cm$^{1/2}$ V$^{-1/2}$) | $\mu_e$ at E=2×10$^5$ V cm$^{-1}$ (cm$^2$ V$^{-1}$ s$^{-1}$) |
|---|---|---|---|
| PBDB-TF | 2.12×10$^{-4}$ | 9.42×10$^{-4}$ | 3.07×10$^{-4}$ |
| PFBCNT10 | 1.20×10$^{-4}$ | 1.53×10$^{-3}$ | 1.21×10$^{-4}$ |
| PFBCNT20 | 7.11×10$^{-4}$ | 9.86×10$^{-4}$ | 7.40×10$^{-4}$ |
| PFBCNT30 | 2.43×10$^{-4}$ | 1.65×10$^{-4}$ | 1.09×10$^{-4}$ |

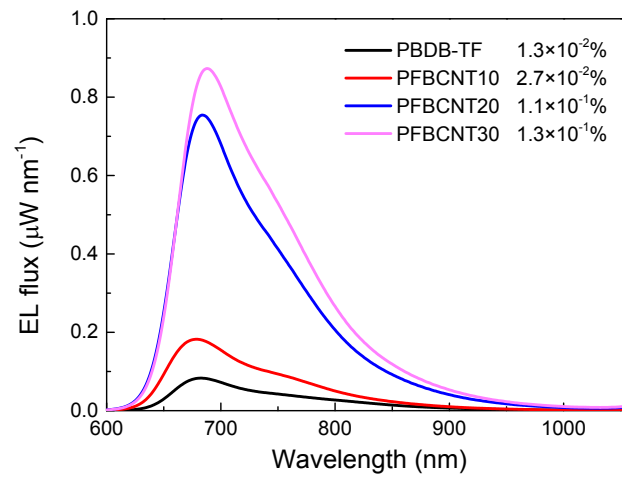**Figure S15.** $J_{sc}$ as the function of $P_{light}$ of the OSCs based on polymer:Y6-BO binary blends.



**Figure S16.** $EQE_{EL}$ spectra of neat polymers.